



# LUND UNIVERSITY

## A Comparison of Ungerboeck and Forney Models for Reduced-Complexity ISI Equalization

Rusek, Fredrik; Loncar, Maja; Prlja, Adnan

*Published in:*

IEEE Global Telecommunications Conference, 2007. GLOBECOM '07.

*DOI:*

[10.1109/GLOCOM.2007.275](https://doi.org/10.1109/GLOCOM.2007.275)

2007

[Link to publication](#)

*Citation for published version (APA):*

Rusek, F., Loncar, M., & Prlja, A. (2007). A Comparison of Ungerboeck and Forney Models for Reduced-Complexity ISI Equalization. In *IEEE Global Telecommunications Conference, 2007. GLOBECOM '07.* (pp. 1431-1436). IEEE - Institute of Electrical and Electronics Engineers Inc..  
<https://doi.org/10.1109/GLOCOM.2007.275>

*Total number of authors:*

3

### General rights

Unless other specific re-use rights are stated the following general rights apply:

Copyright and moral rights for the publications made accessible in the public portal are retained by the authors and/or other copyright owners and it is a condition of accessing publications that users recognise and abide by the legal requirements associated with these rights.

- Users may download and print one copy of any publication from the public portal for the purpose of private study or research.
- You may not further distribute the material or use it for any profit-making activity or commercial gain
- You may freely distribute the URL identifying the publication in the public portal

Read more about Creative commons licenses: <https://creativecommons.org/licenses/>

### Take down policy

If you believe that this document breaches copyright please contact us providing details, and we will remove access to the work immediately and investigate your claim.

LUND UNIVERSITY

PO Box 117  
221 00 Lund  
+46 46-222 00 00

# A Comparison of Ungerboeck and Forney Models for Reduced-Complexity ISI Equalization

Fredrik Rusek, Maja Lončar, Adnan Prlja  
 Dept. of Information Technology, Lund University  
 P. O. Box 118, 22100 Lund, Sweden  
 Email: {fredrikr, maja}@it.lth.se

**Abstract**—This paper investigates the performance of reduced-state trellis-based intersymbol interference equalizers, which are based on the so-called Ungerboeck and Forney observation models. Although the two models are equivalent when an optimum equalizer is employed, their performances differ significantly when using reduced-complexity methods. It is demonstrated that practical equalizers operating on the Forney model outperform those operating on the Ungerboeck model for high signal-to-noise ratios (SNRs), while the situation is reversed for low SNR levels. A novel reduced-complexity equalization strategy that improves on previous Ungerboeck-based equalizers is proposed.

## I. INTRODUCTION

Intersymbol interference (ISI), introduced by a frequency selective communication channel, or by filtering and pulse shaping at the transmitter, requires equalization at the receiver. Since finite ISI can be represented as a finite-state-machine process and thus admits trellis representation, optimum equalization can efficiently be realized using the Viterbi algorithm, or, when soft symbol information is needed (for example, in iterative schemes), the BCJR algorithm.

It is well known that the samples of a filter matched to the receive signal pulse, applied as the receiver front-end, provide sufficient statistics for optimum detection [2]. This is referred to as the Ungerboeck model [1]. Alternatively, the sampled matched filter output can be further processed by a whitening filter, which yields the so-called Forney observation model [2]. Trellis-based equalization can be formulated for both observation models. The choice of the model only affects the metric computation, but the final output of the Viterbi or the BCJR equalizer is identical for both cases. Computational complexity is determined by the number of trellis states. For an ISI channel of memory  $L$  and a modulation alphabet  $\mathcal{M}$ , the trellis has  $|\mathcal{M}|^L$  states with  $|\mathcal{M}|$  branches per state. Thus, for large constellations and/or ISI of high memory, BCJR equalization becomes prohibitively complex. In such scenarios, a suitable alternative are suboptimum algorithms that achieve complexity reduction by effectively reducing the trellis state space. The algorithms that belong to this class are, e.g., the RS-BCJR [3], the T-BCJR [4], the M-BCJR [4] and its improved version [5], and the recently proposed M\*-BCJR [6]. All these methods operate on the Forney model, which is often preferred due to the whiteness of the noise.

This paper investigates the performance of reduced-trellis equalizers that operate on the Ungerboeck model, and compares it with the Forney model. To the best of the authors'

knowledge, there have not been such attempts so far, except in the recent work by Hoehner et al. [7], where the comparison of Ungerboeck and Forney models was conducted for reduced complexity multi-user detectors. The conclusions of [7], however, do not translate to the reduced-trellis ISI equalization we consider here. Among the previously mentioned reduced-trellis methods, the M\*-BCJR algorithm exhibits most advantages and it is therefore chosen as the preferred method in this work.

## II. SYSTEM MODEL

Consider signals  $s(t)$  generated by the linear modulation

$$s(t) = \sum_{k=-\infty}^{\infty} a_k q(t - kT) \quad (1)$$

where  $\mathbf{a} = \dots, a_{-1}, a_0, a_1, \dots$ , is a, possibly encoded, real-valued transmit symbol sequence and  $q(t)$  is a real continuous pulse. It is assumed that  $q(t)$  is a unit energy pulse, that is,  $\int q^2(t)dt = 1$ , which represents the combined effect of the transmit filter and the channel impulse response, generating finite ISI. The signal  $s(t)$  is corrupted by additive white Gaussian noise (AWGN) and the received signal becomes  $r(t) = s(t) + n(t)$ . Forney showed [2] that a set of sufficient statistics to estimate  $\mathbf{a}$  from the linear modulation signal  $r(t)$  is the sequence of the sampled matched filter outputs

$$x_k = \int_{-\infty}^{\infty} r(t)q(t - kT)dt. \quad (2)$$

Inserting the expression for  $r(t)$  into (2) yields

$$x_k = \sum_{l=-L}^L g_l a_{k-l} + \eta_k \quad (3)$$

where

$$g_l = \int_{-\infty}^{\infty} q(t)q(t - lT)dt$$

$$\eta_k = \int_{-\infty}^{\infty} n(t)q(t - kT)dt.$$

In (3) we assume that the autocorrelation coefficients are  $g_l = 0$  for  $|l| > L$ . Eq. (3) is the so-called Ungerboeck observation model, investigated in [1]. The correlation of the noise samples  $\eta_k$  is  $\mathcal{E}\{\eta_k \eta_{k-l}\} = g_l N_0/2$ .

By filtering  $\mathbf{x}$  with a whitening filter, we obtain the sequence  $\mathbf{y}$  given by

$$y_k = \sum_{l=0}^L f_l a_{k-l} + w_k \quad (4)$$

where  $\mathbf{f}$  is a causal ISI  $(L+1)$ -tap long sequence such that  $\mathbf{g}$  is its autocorrelation sequence, and  $w_k$  are independent Gaussian noise samples with variance  $\sigma^2 = N_0/2$ . This is the so-called Forney observation model, also referred to as the whitened matched filter (WMF) model. Due to the whiteness of the noise at the output of the WMF, the Forney model is often preferred to the Ungerboeck model. Since the whitening filter is invertible,  $\mathbf{y}$  also forms a set of sufficient statistics. Thus, the two models have equivalent detection properties. There are many possible whitening filters with the above mentioned properties. The filter that results in a minimum-phase impulse response  $\mathbf{f}$  is most suited for reduced complexity decoding and will be used throughout. Note that for the Forney model (4), at each time  $k$ , the observation  $y_k$  is affected by the current data symbol  $a_k$  and the  $L$  past symbols  $(a_{k-1}, \dots, a_{k-L})$ . In the Ungerboeck model (3), however, each observation  $x_k$  contains not only contributions from the past  $L$  symbols, but also from the future  $L$  symbols. This fundamental difference has a crucial effect on the behavior of reduced-complexity trellis equalizers, as will be explained in Section VII.

### III. OPTIMUM EQUALIZATION

The maximum *a posteriori* (MAP) sequence equalizer outputs

$$\hat{\mathbf{a}} = \arg \max_{\mathbf{a}} p(\mathbf{a}|\mathbf{x}) = \arg \max_{\mathbf{a}} p(\mathbf{a}|\mathbf{y})$$

where  $p(\mathbf{a}|\mathbf{x}) \propto p(\mathbf{x}, \mathbf{a}) = p(\mathbf{x}|\mathbf{a})p(\mathbf{a})$ . Assuming independent data symbols, the *a priori* sequence probability factorizes into  $p(\mathbf{a}) = \prod_k p(a_k)$ . In the Forney observation model, the received sequence  $\mathbf{y}$  contains i.i.d. noise samples, which allows factorization

$$p(\mathbf{y}|\mathbf{a}) = \prod_k p(y_k|\mathbf{a})$$

where  $p(y_k|\mathbf{a}) \propto \exp\left[-\frac{1}{N_0}\left(y_k - \sum_{l=0}^L f_l a_{k-l}\right)^2\right]$ . (5)

Then, the Viterbi branch metric at  $k$ th trellis stage is proportional to  $p(a_k)p(y_k|\mathbf{a})$ .

In the Ungerboeck model, the observed matched-filter output  $\mathbf{x}$  is corrupted by colored noise, thus, the above factorization does not hold. However,  $p(\mathbf{x}|\mathbf{a})$  can be factorized [1], which allows application of the Viterbi algorithm,

$$p(\mathbf{x}|\mathbf{a}) \propto \prod_k \varphi(x_k, \mathbf{a})$$

where  $\varphi(x_k, \mathbf{a})$ , however, is not a probability density function (PDF) [8], and it is given by

$$\varphi(x_k, \mathbf{a}) \triangleq \exp\left[\frac{2}{N_0}\left(x_k a_k - \frac{g_0}{2} a_k^2 - \sum_{l=1}^L g_l a_k a_{k-l}\right)\right]. \quad (6)$$

The MAP symbol equalizer outputs the most probable symbol  $\hat{a}_k$ , for each time instant  $k$ ,

$$\hat{a}_k = \arg \max_{a_k} p(a_k|\mathbf{x}) = \arg \max_{a_k} p(a_k|\mathbf{y}).$$

Additionally, it provides soft symbol reliabilities, expressed in terms of logarithmic *a posteriori* probability (APP) ratios

$$L(a_k) \triangleq \log \frac{p(a_k = +1|\mathbf{x})}{p(a_k = -1|\mathbf{x})} = \log \frac{\sum_{\mathbf{a}: a_k = +1} p(\mathbf{a}|\mathbf{x})}{\sum_{\mathbf{a}: a_k = -1} p(\mathbf{a}|\mathbf{x})} \quad (7)$$

where, for simplicity, we assume bipolar signalling. Let  $\mathcal{S}_k^+$  and  $\mathcal{S}_k^-$  denote sets of state pairs  $(s_k, s_{k+1})$  in the underlying trellis that correspond to the  $k$ th transmit symbol equal to  $a_k = +1$  and  $a_k = -1$ , respectively. For time-invariant trellises, time index can be omitted, that is,  $\mathcal{S}_k^- = \mathcal{S}^-$  and  $\mathcal{S}_k^+ = \mathcal{S}^+$ . Then, the log-APP ratio (7) can be rewritten as

$$L(a_k) = \log \frac{\sum_{(s,s') \in \mathcal{S}^+} p(s_k = s, s_{k+1} = s', \mathbf{x})}{\sum_{(s,s') \in \mathcal{S}^-} p(s_k = s, s_{k+1} = s', \mathbf{x})}. \quad (8)$$

The BCJR algorithm efficiently computes the log-APP ratios using the factorization

$$p(s_k = s, s_{k+1} = s', \mathbf{x}) = \alpha_k(s) \gamma_k(s, s') \beta_{k+1}(s') \quad (9)$$

where  $\alpha_k(s)$  is the forward metric of the state  $s$  at  $k$ th trellis depth,  $\beta_{k+1}(s')$  is the backward metric of the state  $s'$  at depth  $k+1$ , and  $\gamma_k(s, s')$  is the metric of the branch connecting the states  $(s, s')$ . The forward metric is computed recursively in a forward trellis sweep according to

$$\alpha_{k+1}(s') = \sum_{s \in \mathcal{S}} \alpha_k(s) \gamma_k(s, s') \quad (10)$$

with the initialization  $\alpha_0(0) = 1$ , and  $\alpha_0(s) = 0$ , for  $s \neq 0$ . Similarly, the backward recursion starts at the end of the trellis and proceeds towards the root of the trellis computing at each depth

$$\beta_k(s) = \sum_{s' \in \mathcal{S}} \beta_{k+1}(s') \gamma_k(s, s'). \quad (11)$$

In the Forney observation model, the branch metric is

$$\gamma_k(s, s') = p(s, y_k | s') = p(a_k) p(y_k | \mathbf{a})$$

where  $p(y_k | \mathbf{a})$  is given by (5). The state metrics are the probability functions  $\alpha_k(s) = p(s, \mathbf{y}_{[0,k]})$ ,  $\beta_{k+1}(s) = p(\mathbf{y}_{[k+1,K]} | s)$ , where  $\mathbf{y}_{[a,b]} = (y_a y_{a+1} \dots y_{b-1})$ .

For the Ungerboeck model, the probabilistic interpretation of the BCJR metrics is no longer valid. However, it was shown in [8] that the factorization (9) is also possible, with

$$\gamma_k(s, s') = p(a_k) \varphi(x_k, \mathbf{a})$$

where  $\varphi(x_k, \mathbf{a})$  is a function given by (6). This enables the implementation of the BCJR algorithm with the same recursions for  $\alpha_k(s)$ ,  $\beta_{k+1}(s')$  as before, cf. (10) and (11).

### IV. THE M\*-BCJR ALGORITHM

The M\*-BCJR algorithm [6], computes the L-values (7) in the same manner as the BCJR algorithm; however, similarly as in the M-BCJR [4], at each trellis stage in the forward recursion only  $M$  states with the highest forward metric are retained. Unlike in the M-BJCR, the remaining states are not deleted, but rather merged with the surviving states. Merging of two states implies that their forward metrics are summed up and the branches of the inferior state are redirected into the surviving state. Such a modified trellis is subsequently used in the backward recursion. Although merging the states slightly increases the complexity, it preserves the balance of the branches that carry opposite symbols at each trellis depth, and thus avoids problems when computing the L-values.

Since a state is an  $L$ -tuple  $(a_{k-1} \dots a_{k-L})$  of the most recent  $L$  symbols, then two states that differ in  $t \leq L$  ending positions merge in the trellis after  $t$  steps. If  $t$  is small, the metric difference of the paths leading to the common state is supposed not to be large [6]. If  $\mathcal{S}_M$  and  $\mathcal{S}_{\mathcal{M}}$  denote the set of the  $M$  best states and the set of the remaining states at a certain depth, respectively, then a rule proposed in [6] is that a state  $s' \in \mathcal{S}_{\mathcal{M}}$  is merged with such a state  $s \in \mathcal{S}_M$  that differs in the least number  $t$  of the ending positions. In the next subsection, we discuss realization of this merging rule in more detail and also propose alternative merging strategies. Hereinafter, we assume binary representation of the states ( $L \log_2(|\mathcal{M}|)$  bits).

### State Merging Strategies

1) If  $\oplus$  denotes the bitwise x-or operator, then the zero bits in  $s \oplus s'$  indicate the positions where the states  $s$  and  $s'$  coincide. The state merging can be efficiently realized in the following way: for each state  $s' \in \mathcal{S}_{\mathcal{M}}$  compute the values  $s \oplus s'$  for all  $s \in \mathcal{S}_M$ ; find the state  $s$  which yields the smallest value of  $s \oplus s'$  (interpreted as a decimal number), and merge  $s'$  with  $s$ . We refer to this merging rule as  $\mathcal{R}_1$ . It ensures that  $s' \in \mathcal{S}_{\mathcal{M}}$  will be merged with the state  $s \in \mathcal{S}_M$  that coincides with  $s'$  in the largest number of leading positions. In case of a tie, a state with the smaller value of  $s \oplus s'$  is preferred.

2) A modified approach, which we denote  $\mathcal{R}_2$ , resolves the above mentioned cases of a tie, in a different way. As in  $\mathcal{R}_1$ , a state  $s' \in \mathcal{S}_{\mathcal{M}}$  is merged with the state  $s \in \mathcal{S}_M$  with the largest number of coinciding leading positions; however, if there is more than one such state in  $\mathcal{S}_M$ , then we choose the one with the *smallest value of the forward metric*. Good results obtained with this merging strategy, indicate that the metric values should be taken into account when merging the states.

3) Motivated by the previous observation, we propose strategy  $\mathcal{R}_3$ , which is simply to merge *all* the states from  $\mathcal{S}_{\mathcal{M}}$  with the state  $s \in \mathcal{S}_M$  that has the smallest forward metric. Note that this strategy is the simplest to implement, since it does not require any additional computations or sorting procedures during the merging process, unlike the previous two.

We have also tested replacing the "smallest-metric" choice in  $\mathcal{R}_2$  and  $\mathcal{R}_3$  by the "largest metric"; however, this variant of the algorithm fails completely. This suggests that, among the chosen  $M$  states at each stage, the "good" states with large metric should be left intact, while the "weak" states should be used to "collect" the discarded states from  $\mathcal{S}_{\mathcal{M}}$ .

We have tested approaches  $\mathcal{R}_1$ ,  $\mathcal{R}_2$ , and  $\mathcal{R}_3$  with various ISI patterns. The rules  $\mathcal{R}_2$  and  $\mathcal{R}_3$  outperform  $\mathcal{R}_1$ , allowing largest complexity reduction, that is, the smallest  $M$ , to reach the specified bit error rate (BER). For a given value of  $M$ ,  $\mathcal{R}_2$  yields the lowest BER, and it will therefore be used hereinafter.

## V. RECEIVER TESTS

### A. M\*-BCJR Equalizer for Uncoded ISI

Consider first uncoded BPSK transmission over an ISI channel of memory  $L$ . The complexity of the BCJR equalizer is of the order  $2^L$ . In our tests, we have used two standard ISI channel models, both causing severe ISI, and both of memory

$L = 4$ : the minimum-phase equivalent of the Proakis-C channel, with taps  $\mathbf{f} = (0.2448 \ 0.4774 \ 0.6868 \ 0.4428 \ 0.2106)$ , and the channel  $\mathbf{f} = (\sqrt{0.45} \ \sqrt{0.25} \ \sqrt{0.15} \ \sqrt{0.1} \ \sqrt{0.05})$  used in [6] and [9]. All the results presented here are given for the Proakis-C channel only, due to space limitations, with the note that all the observations hold for the other channel as well. The bit error rate performances of the M\*-BCJR equalizers, based on the two observation models, with  $M = 4$  states, employing the merging rule  $\mathcal{R}_2$ , are shown in Figure 1. As a reference, the performance of the BCJR equalizer (with  $M = 16$  states) is also shown. It is observed that the Forney-based M\*-BCJR follows the BCJR performance with a small loss, while the Ungerboeck-based equalizer completely fails for the medium and high signal-to-noise ratio (SNR) levels, suffering from a high error floor. This error floor is eliminated only when the number of preserved states  $M$  approaches the full-complexity value  $M = 16$ . In the low SNR region, however, left from the crossover point at  $E_s/N_0 \approx 2.5$  dB, the behavior is reversed and the Ungerboeck model yields lower BER than the Forney model. Further insights regarding these observations will be provided in the next section.

### B. Turbo Equalization for Coded ISI

Consider coded transmission over an ISI channel, as depicted in Figure 2. After coding and interleaving, the data sequence is mapped to the symbol constellation and transmitted over an ISI channel. This scheme can be viewed as serially concatenated coding, where the mapper and the ISI channel act as an inner encoder. Thus, the iterative principle for equalization and decoding can be applied at the receiver, cf. Figure 3, as first proposed in [9].

We have used the M\*-BCJR equalizer as inner decoder in the turbo scheme, with the channel parameters from the previous subsection. A memory 1 convolutional code with the generator matrix  $(1 + D, 1) = (6, 4)_8$  was used as the outer code, and the block length was 1000 information bits. The BER performance of the scheme is shown in Figure 4, for two choices of  $M$ , with the benchmark given by the

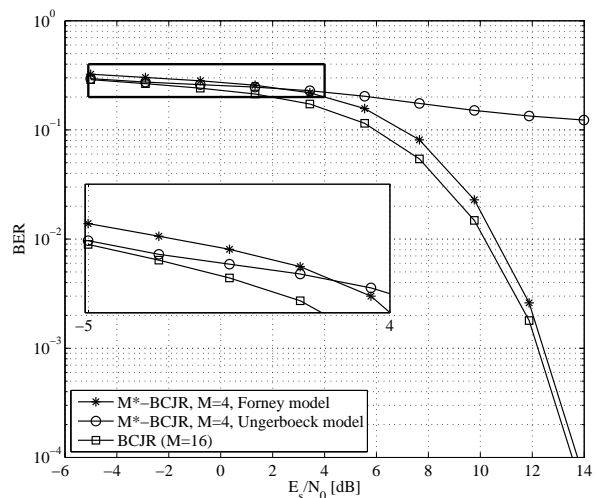


Fig. 1. Bit error rate performance of the Forney- and Ungerboeck-based M\*-BCJR equalizers with  $M = 4$ , for Proakis-C 5-tap ISI channel.

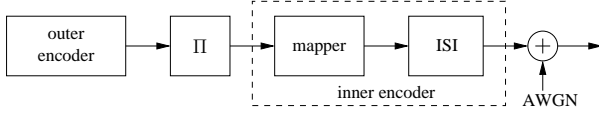


Fig. 2. Communication system with coding and intersymbol interference

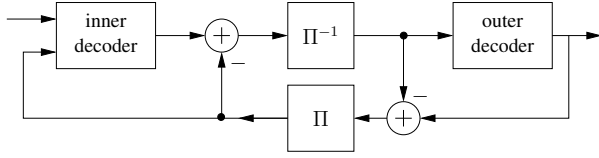


Fig. 3. Iterative receiver structure

turbo BCJR equalizer and the underlying outer code. For both  $M = 4$  and  $M = 6$  we observe a crossover of the BER curves corresponding to the Forney- and Ungerboeck-based equalizers. The weaker outer code was chosen deliberately in order to obtain crossover points in Figure 4 at moderate BER. Note that the SNR range in Figure 4 corresponds to the left-hand half of the equalizer's operating range considered in Figure 1, where the difference between the two models is not as drastic as in the right-hand half. We conclude from Figure 4 that the Ungerboeck-based M\*-BCJR equalization is preferred for very low SNRs, while the Forney model yields lower BER for higher SNR. In other words, for a given SNR in the high SNR region, a certain BER can be achieved with the Forney model with lower complexity (smaller  $M$ ) than with the Ungerboeck model.

## VI. PERFORMANCE EVALUATION VIA MUTUAL INFORMATION

To analyze the BER behavior of the uncoded and coded systems tested above, we use the mutual information  $I_A = I(\mathbf{a}; L(\mathbf{a}))$  between the sequence of the L-values  $L(\mathbf{a})$  at the output of the equalizer and the transmitted sequence  $\mathbf{a}$ . Analytical computation of  $I_A$  is far too difficult in practice. Instead,

assuming independence of  $a_k$ , we consider the marginal PDF of the equalizer output,

$$f(l|\alpha) \triangleq f(L(a_k) = l | a_k = \alpha), \quad (12)$$

and use it to compute  $I(\mathbf{a}; L(\mathbf{a}))$ . For ISI channels with bipolar equiprobable inputs, the PDF satisfies  $f(l|1) = f(-l|-1)$ . The mutual information can be computed by solving the integral

$$I_A = 1 - \int_{-\infty}^{\infty} f(l|1) \log_2(1 + e^{-l}) dl. \quad (13)$$

This integral is solved numerically, using the empirical estimate of the marginal density  $f(l|1)$ : an observation sequence  $\mathbf{y}$  (or  $\mathbf{x}$ ) is formed from  $3 \times 10^7$  information bits, the equalizer under investigation is then applied to this sequence (without any *a priori* information) and a histogram of all  $L(a_k)$  where  $a_k = 1$  is used to estimate  $f(l|1)$ .

Figure 5 illustrates the information  $I_A$  for the setups considered in Figures 1 and 4. It is clearly seen that for high SNR, the mutual information obtained with the Ungerboeck model is below that obtained with the Forney model. For  $M = 4$ , the Forney-based equalizer shows rather good performance in the high SNR region, close to the BCJR, but the Ungerboeck-based method performs poorly. For very low SNR, the Ungerboeck model yields higher  $I_A$  than the Forney model. The crossover point between the Forney and Ungerboeck models in Figure 5 corresponds rather well to the BER crossover points in Figures 1 and 4. The BER in Figure 1 equals  $\text{BER} = \int_{-\infty}^0 f(l|1) dl$ , while the mutual information is given by (13), thus there cannot be an exact agreement between the crossover points. For  $M = 4$ , the crossover in the iterative receiver test occurs at  $E_s/N_0 = 3.1$  dB, while the mutual information chart suggests that it should occur at  $E_s/N_0 = 3.5$  dB.

In the analysis of the iterative equalization process, it is not sufficient to consider only  $I_A$ . The mutual information  $I_A$  is only involved in the first iteration; in subsequent iterations, influence of *a priori* information must be considered – this is

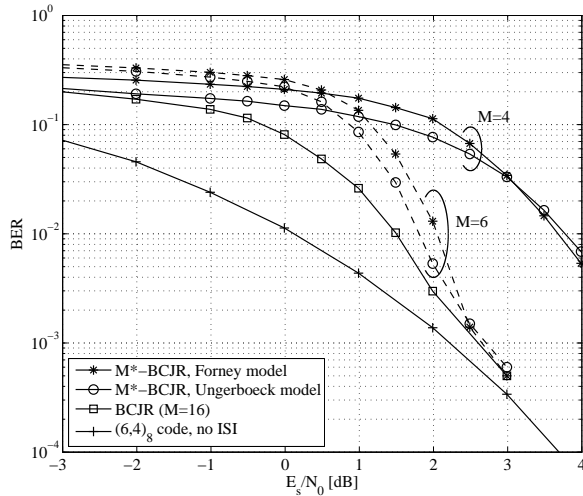


Fig. 4. Performance of the Forney- and Ungerboeck-based M\*-BCJR equalizers in a turbo scheme, after 8 iterations, for Proakis-C 5-tap ISI channel, and a memory 1, rate 1/2 outer convolutional code.

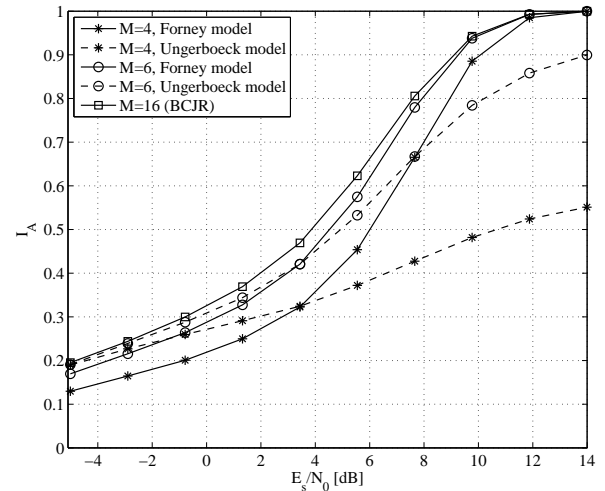


Fig. 5. Mutual information between the output of the M\*-BCJR algorithm and the transmitted symbol sequence. Dashed curves correspond to the Ungerboeck model and the solid ones to the Forney model.

the well known EXIT chart technique. However,  $I_A$  predicts the BER performance of the turbo equalizer quite well, which will be explained in the following. If  $T_{\text{ISI}}(x)$  denotes the EXIT curve for the ISI channel, then there is the following analogy between  $I_A$  and  $T_{\text{ISI}}(x)$ : if a certain equalizer and ISI model is better than another one, then  $T_{\text{ISI}}(x) > T'_{\text{ISI}}(x)$ ,  $0 \leq x \leq 1$ , instead of  $I_A > I'_A$  for the uncoded case. The starting point of  $T_{\text{ISI}}(x)$  is  $T_{\text{ISI}}(0) = I_A$ , while the ending point is, as shown in [10],  $T_{\text{ISI}}(1) = T_{\text{MLC}}(0)$ , where 'MLC' denotes 'memoryless channel' (in fact,  $T_{\text{MLC}}(0) = T_{\text{MLC}}(x)$ ,  $0 < x \leq 1$ ). Thus, the endpoints of all EXIT curves are the same, and their starting points are determined by  $I_A$ . Therefore, when  $I_A > I'_A$ , it is plausible that  $T_{\text{ISI}}(x) > T'_{\text{ISI}}(x)$ ,  $0 \leq x \leq 1$  as well. This explains the good match between  $I_A$  and the BER performance of the turbo equalization.

Although  $I_A$  is much larger at higher SNR for the M\*-BCJR equalizer based on the Forney model than for the one based on the Ungerboeck model, it is not possible to conclude that in general the Forney-based equalization is superior to the Ungerboeck-based one. The difference in  $I_A$  may be a consequence of the M\*-BCJR algorithm itself, which approximates L-values with reduced complexity. There are two approximations involved: (i) the L-values are computed with only  $M$  nonzero values  $\alpha_k(s)$  at every depth  $k$ , and (ii) these  $M$  nonzero  $\alpha_k(s)$  are not computed with full complexity, but they are themselves only approximations.

## VII. GENIE-AIDED EQUALIZERS

In order to eliminate approximations (ii) from the above discussion, a genie-aided equalizer, denoted by  $\mathcal{G}_1$ , is considered next. A genie provides the exact values of  $\alpha_k(s)$  and  $\beta_k(s)$  for all depths  $k$ . The L-values  $L(a_k)$  are computed using the  $M$  largest values  $\alpha_k(s)$  only. This method serves as a benchmark for equalizers that construct a reduced trellis in the forward recursion based on the largest  $\alpha_k(s)$ . The mathematical formulation of  $\mathcal{G}_1$  is as follows: Define  $\delta_k$  as the  $M$ th largest metric  $\alpha_k(s)$  at depth  $k$ , and

$$\hat{\alpha}_k(s) \triangleq \begin{cases} \alpha_k(s), & \alpha_k(s) \geq \delta_k \\ 0, & \alpha_k(s) < \delta_k. \end{cases} \quad (14)$$

The values  $L(a_k)$  are obtained as in (8) but with

$$p(s_k = s, s_{k+1} = s', \mathbf{x}) = \hat{\alpha}_k(s) \gamma_k(s, s') \beta_{k+1}(s). \quad (15)$$

Figure 6 shows the mutual information obtained with the genie-aided equalizer  $\mathcal{G}_1$ , for the same parameters as in Figure 5. It is readily seen that, even with  $\mathcal{G}_1$ , the Ungerboeck model still performs poorly in the high SNR region. Moreover, for a given  $M$ , the Forney curve lies strictly above the Ungerboeck curve, which implies the conclusion that equalizers which construct reduced trellis in the forward recursion (based on the largest  $\alpha_k(s)$ ), should operate on the Forney model.

Since the equalizer  $\mathcal{G}_1$  does not perform well with the Ungerboeck model, we next consider a more general class of equalizers. These equalizers build two independent reduced trellises: one in the forward recursion, based on the largest  $\alpha$ -metric, and one in the backward recursion, based on the largest

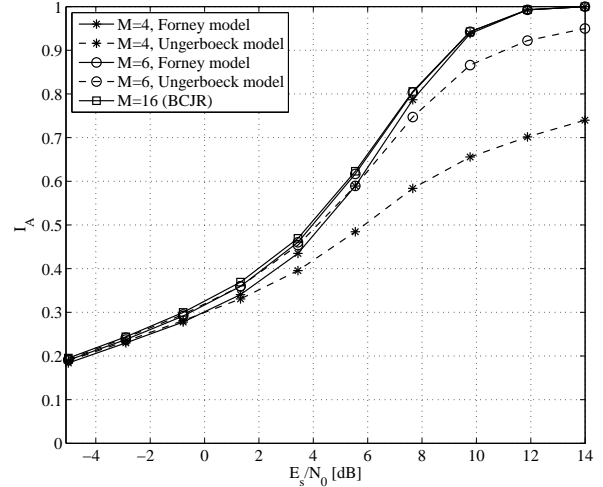


Fig. 6. Outcome of the genie-aided equalizer  $\mathcal{G}_1$ . Dashed curves correspond to the Ungerboeck model and the solid ones to the Forney model.

$\beta$ -metric. The L-values are obtained from the union of the two trellises (explained formally below). Such equalizers have been investigated earlier in [5]. A genie-aided equalizer  $\mathcal{G}_2$ , which is a benchmark for this class, is considered. The genie provides all exact  $\alpha_k(s)$  and  $\beta_k(s)$  values (computed with full complexity). For each trellis stage  $k$ , define  $\hat{\alpha}_k(s)$  according to (14) and  $\hat{\beta}_k(s)$  similarly. The branches that are involved in the computation of  $L(a_k)$  are those that have at least one endpoint with nonzero metric  $\hat{\alpha}_k(s)$  or  $\hat{\beta}_k(s)$ . If a certain branch has both endpoints with nonzero  $\hat{\alpha}_k(s)$  and  $\hat{\beta}_k(s)$ , its contribution to  $L(a_k)$  becomes  $\hat{\alpha}_k(s) \gamma_k(s, s') \hat{\beta}_{k+1}(s)$ . If, however, a branch has only one nonzero endpoint, the genie provides the necessary ("missing")  $\alpha_k(s)$  or  $\beta_k(s)$  value, and the contribution becomes  $\hat{\alpha}_k(s) \gamma_k(s, s') \beta_{k+1}(s)$  or  $\alpha_k(s) \gamma_k(s, s') \hat{\beta}_{k+1}(s)$ . For practical equalizers of this type, where genie knowledge is not available, the contribution of such branches is not clearly defined. In [5] it was proposed how to handle these cases in practice and compensate for the "missing" endpoint metrics.

The tests show that the outcome of the equalizer  $\mathcal{G}_2$  is, in terms of the mutual information  $I_A$ , virtually identical to that of  $\mathcal{G}_1$ , cf. Figure 6. Thus, this approach does not seem to benefit from the Ungerboeck model either.

In order to understand and solve the weakness of equalization strategies based on the Ungerboeck model, we take a step back and consider the function  $\varphi(x_k, \mathbf{a})$ , given by (6), which defines the BCJR branch metric. Assuming bipolar signaling and a unit energy ISI response, (6) can be written as

$$\varphi(x_k, \mathbf{a}) = \exp \left\{ \frac{2}{N_0} \left[ a_k \left( x_k - \sum_{l=1}^L g_l a_{k-l} \right) - \frac{1}{2} \right] \right\}. \quad (16)$$

For an arbitrary state at depth  $k$ , the  $\varphi$  values associated with the outgoing branches for  $a_k = 1$  and  $a_k = -1$  are  $e^{(2\mu-1)/N_0}$  and  $e^{(-2\mu-1)/N_0}$ , respectively, where  $\mu = x_k - \sum_{l=1}^L g_l a_{k-l}$ . The received signal at time instant  $k$  can be written as

$$x_k = \tilde{a}_k + \sum_p + \sum_f + \eta_k, \quad (17)$$

where  $\tilde{\mathbf{a}}$  is the actual transmitted symbol sequence;  $\Sigma_p$  and  $\Sigma_f$  are the contributions to  $x_k$  from past and future symbols. The correct path in the trellis (corresponding to the transmitted sequence  $\tilde{\mathbf{a}}$ ) passes through the state  $s = (\tilde{a}_{k-1} \dots \tilde{a}_{k-L})$  at time point  $k$ . This implies that the sum  $\sum_{l=1}^L g_l a_{k-l}$  in (16) is equal to the term  $\Sigma_p$  in (17). Thus,  $\varphi(x_k, \mathbf{a})$  equals

$$\varphi(x_k, \mathbf{a}) = \exp \left\{ \frac{2}{N_0} \left[ a_k (\tilde{a}_k + \Sigma_f + \eta_k) - \frac{1}{2} \right] \right\}. \quad (18)$$

In the high SNR region, where the Ungerboeck model shows poor performance, the approximation  $\eta_k \approx 0$  holds. If the term  $\Sigma_f$  was not present, the two outgoing branches, corresponding to  $a_k = \tilde{a}_k$  and  $a_k = -\tilde{a}_k$  would have the metric  $\varphi \propto e^{1/N_0}$  and  $\varphi \propto e^{-1/N_0}$ , respectively, and thus the correct path gets a much larger metric value. But, when  $\sum_{l=1}^L g_l > 1$ , which corresponds to the closed eye diagram<sup>1</sup>, it is possible that  $|\Sigma_f| > 1$ , which implies that  $\tilde{a}_k + \Sigma_f$  can have the sign opposite from  $\tilde{a}_k$ . This leads to the incorrect path (with  $a_k = -\tilde{a}_k$ ) having a larger metric at time step  $k+1$ , than the correct path (with  $a_k = \tilde{a}_k$ ). Note that this happens without any noise and that there is a constant probability for this to occur. The correct state at time  $k+1$ , corresponding to  $a_k = \tilde{a}_k$ , would then have a small metric  $\alpha_{k+1}(s)$  and would likely be eliminated from the list. Thus, the correct path in the trellis would be lost, and cannot be recovered. Therefore, we propose to always include both states (corresponding to  $a_k = \pm 1$ ) into the set of  $M$  surviving states at time  $k+1$ .

The method described above is formally expressed next. Partition the state space  $\mathcal{S}$  as  $\mathcal{S} = \{\mathcal{P}_1, \dots, \mathcal{P}_{2^L-1}\}$ , where each set  $\mathcal{P}_l$  holds a pair of states  $(s, s')$  such that if  $(\tilde{s}, s) \in \mathcal{S}^+$  for some state  $\tilde{s} \in \mathcal{S}$ , then  $(\tilde{s}, s') \in \mathcal{S}^-$ . Define  $\alpha_{\max,k}^l \triangleq \max\{\alpha_k(s), \alpha_k(s')\}$ ,  $(s, s') \in \mathcal{P}_l$ , and define  $\delta_k$  as the  $(M/2)$ th largest metric  $\alpha_{\max,k}^l$  at each depth  $k$ ;  $M$  is assumed to be an even integer. Then the survivor states are all states that have nonzero  $\hat{\alpha}_k(s)$ , where

$$\hat{\alpha}_k(s) \triangleq \begin{cases} \alpha_k(s), & \alpha_{\max,k}^l \geq \delta_k, s \in \mathcal{P}_l \\ 0, & \text{otherwise.} \end{cases} \quad (19)$$

The outcome of this approach, denoted by  $\mathcal{G}_3$ , based on the Ungerboeck model is shown in Figure 7. The performance of  $\mathcal{G}_3$  is much better than that of  $\mathcal{G}_1$  and  $\mathcal{G}_2$ . The method works very well even with only two survivor states per depth.

The reduced trellis construction of  $\mathcal{G}_3$  can be incorporated into the  $M^*$ -BCJR to obtain a new practical equalizer. However, its performance is not as good as one would expect from Figure 7. In fact, its mutual information  $I_A$  is below that of the original  $M^*$ -BCJR algorithm shown in Figure 5. How to exploit the gain promised by  $\mathcal{G}_3$  is a topic for future research.

## VIII. SUMMARY AND CONCLUSIONS

In this paper we have compared the performance of reduced complexity equalizers based on the Forney and the Ungerboeck observation models. It was demonstrated that in the very low SNR region, the Ungerboeck model is preferred for

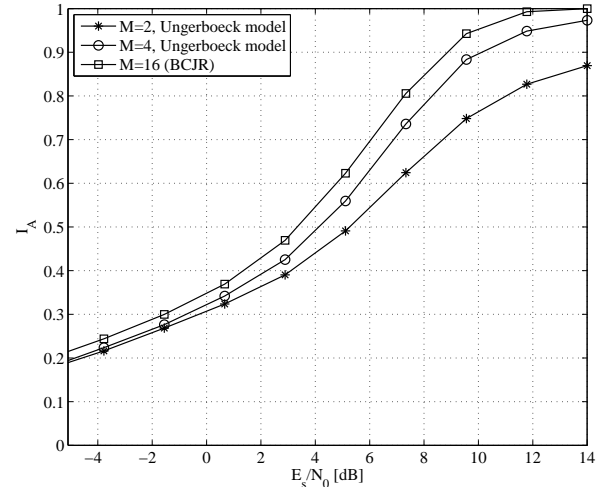


Fig. 7. Outcome of the genie-aided equalizer  $\mathcal{G}_3$  based on the Ungerboeck model.

practical equalizers. But, as the SNR increases, equalization based on the Forney model performs remarkably better. To investigate the ultimate performance of standard equalizers, a genie-aided reduced-trellis equalizer was considered; it also shows the weakness of Ungerboeck-based reduced-complexity equalization for high SNR. A new genie-aided equalizer is constructed for the Ungerboeck model, that succeeds in reaching the performance of the Forney-based equalizer.

## ACKNOWLEDGMENT

This work was supported in part by the Royal Swedish Academy of Sciences and in part by the Swedish Research Council under Grants 621-2004-4703 and 621-2003-3210.

## REFERENCES

- [1] G. Ungerboeck, "Adaptive maximum-likelihood receiver for carrier-modulated data-transmission systems," *IEEE Trans. Commun.*, vol. 22, no. 5, pp. 624–636, May 1974.
- [2] G. D. Forney, Jr., "Maximum-likelihood sequence estimation of digital sequences in the presence of intersymbol interference," *IEEE Trans. Inform. Theory*, vol. 18, no. 2, pp. 363–378, May 1972.
- [3] G. Colavolpe, G. Ferrari, and R. Raheli, "Reduced-state BCJR-type algorithms," *IEEE J. Select. Areas Commun.*, vol. 19, no. 5, pp. 848–859, May 2001.
- [4] V. Franz and J. B. Anderson, "Concatenated decoding with a reduced-search BCJR algorithm," *IEEE Trans. Commun.*, vol. 16, no. 2, pp. 186–195, Feb. 1998.
- [5] C. Fragouli, N. Seshadri, and W. Turin, "On the reduced trellis equalization using the M-BCJR algorithm," in *Proc. Conf. Inform. Sciences and Systems*, Princeton University, USA, Mar. 2000.
- [6] M. Sikora and D. J. Costello, Jr., "A new SISO algorithm with application to turbo equalization," in *Proc. IEEE Int. Symp. Inform. Theory*, Adelaide, Australia, 2005.
- [7] S. Badri-Hoehner, P. A. Hoeher, H. Chen, C. Krakowski, and W. Xu, "Ungerboeck metric versus Forney metric in reduced-state multi-user detectors," in *Proc. 4th Int. Symp. Turbo Codes & Related Topics*, Munich, Germany, 2006.
- [8] G. Colavolpe and R. Barbieri, "On MAP symbol detection for ISI channels using the Ungerboeck observation model," *IEEE Commun. Letters*, vol. 9, no. 8, pp. 720–722, Aug. 2005.
- [9] C. Douillard, A. Picart, P. Didier, M. Jzquel, C. Berrou, and A. Glavieux, "Iterative correction of intersymbol interference: turbo-equalization," *European Trans. Telecomm.*, vol. 6, no. 5, pp. 507–512, 1995.
- [10] F. Rusek and J. Anderson, "Serial and parallel concatenations based on faster-than-Nyquist signaling," in *Proc. IEEE Int. Symp. Inform. Theory*, Seattle, USA, July 2006, pp. 970–974.

<sup>1</sup>The standard notation for closed eye is  $2 \sum_{l=1}^L g_l > 1$ .